



RETRACTED: Hepatoma Cell-Derived Extracellular Vesicles Promote Liver Cancer Metastasis by Inducing the Differentiation of Bone Marrow Stem Cells Through microRNA-181d-5p and the FAK/Src Pathway

OPEN ACCESS

Edited by:

Zhengfei Zhu,
Fudan University, China

Reviewed by:

Yu Ota,
Asahikawa Medical University, Japan
Tatiana Lopatina,
University of Turin, Italy

***Correspondence:**

Jian Pu
pujian0929@163.com

[†]These authors have contributed
equally to this work and share
first authorship

Specialty section:

This article was submitted to
Molecular and Cellular Oncology,
a section of the journal
*Frontiers in Cell and Developmental
Biology*

Received: 16 September 2020

Accepted: 08 February 2021

Published: 28 May 2021

Citation:

Wei H, Wang J, Xu Z, Li W, Wu X, Zhuo C, Lu Y, Long X, Tang Q and Pu J (2021) Hepatoma Cell-Derived Extracellular Vesicles Promote Liver Cancer Metastasis by Inducing the Differentiation of Bone Marrow Stem Cells Through microRNA-181d-5p and the FAK/Src Pathway. *Front. Cell Dev. Biol.* 9:607001. doi: 10.3389/fcell.2021.607001

Huamei Wei^{1,2†}, Jianchu Wang^{2,3†}, Zuoming Xu^{2,3†}, Wenchuan Li^{2,3}, Xianjian Wu², Chenyi Zhuo⁴, Yuan Lu², Xidai Long^{1,2}, Qianli Tang^{2,3} and Jian Pu^{2,3*}

¹ Department of Pathology, The Affiliated Hospital of Youjiang Medical University for Nationalities, Guangxi, China, ² Clinic Medicine Research Center of Hepatobiliary Diseases, Guangxi, China, ³ Department of Hepatobiliary Surgery, The Affiliated Hospital of Youjiang Medical University for Nationalities, Guangxi, China, ⁴ Graduate College of Youjiang Medical University for Nationalities, Guangxi, China

Bone marrow mesenchymal stem cells (BMSCs) are beneficial to repair the damaged liver. Tumor-derived extracellular vesicles (EV) are notorious in tumor metastasis. But the mechanism underlying hepatoma cell-derived EVs in BMSCs and liver cancer remains unclear. We hypothesize that hepatoma cell-derived EVs compromise the effects of BMSCs on the metastasis of liver cancer. The differentially expressed microRNAs (miRNAs) were screened. HepG2 cells were transfected with miR-181d-5p mimic or inhibitor, and the EVs were isolated and incubated with BMSCs to evaluate the differentiation of BMSCs into fibroblasts. Hepatoma cells were cultured with BMSCs conditioned medium (CM) treated with HepG2-EVs to assess the malignant behaviors of hepatoma cells. The downstream genes and pathways of miR-181d-5p were analyzed and their involvement in the effect of EVs on BMSC differentiation was verified through functional rescue experiments. The nude mice were transplanted with BMSCs-CM or BMSCs-CM treated with HepG2-EVs, and then tumor growth and metastasis *in vivo* were assessed. HepG2-EVs promoted fibroblastic differentiation of BMSCs, and elevated levels of α -SMA, vimentin, and collagen in BMSCs. BMSCs-CM treated with HepG2-EVs stimulated the proliferation, migration, invasion and epithelial-mesenchymal-transition (EMT) of hepatoma cells. miR-181d-5p was the most upregulated in HepG2-EVs-treated BMSCs. miR-181d-5p targeted SOCS3 to activate the FAK/Src pathway and SOCS3 overexpression inactivated the FAK/Src pathway. Reduction of miR-181d-5p in HepG2-EVs or SOCS3 overexpression reduced the differentiation of BMSCs into fibroblasts, and compromised the promoting effect

of HepG2-EVs-treated BMSCs-CM on hepatoma cells. *In vivo*, HepG2-EVs-treated BMSCs facilitated liver cancer growth and metastasis. In conclusion, HepG2-EVs promote the differentiation of BMSCs, and promote liver cancer metastasis through the delivery of miR-181d-5p and the SOCS3/FAK/Src pathway.

Keywords: liver cancer, extracellular vesicles, bone marrow mesenchymal stem cells, metastasis, microRNA-181d-5p, epithelial-mesenchymal-transition, FAK/Src pathway

INTRODUCTION

Liver cancer is the sixth most common cancer in the world, with over 840,000 new cases in 2018 (Kontogiannis and MacDaragh Ryan, 2020). In contrast to the overall decline of four major cancers (lung, breast, prostate and colorectal cancer), the mortality rate of liver cancer increased by 2.7% per year in women and 1.6% per year in men between 2011 and 2015 (Jemal, 2018). Administration of sorafenib is the most accepted option for hepatocellular carcinoma (HCC) patients in late-stage cases and in intermediate stage with portal vein thrombosis (Rudolph and Reddy, 2008). However, fewer than 1/3 of the patients benefit from it and show evident drug resistance, toxicity and inefficacy, and other side-effects within 6 months after the regimen (Singh, 2020). In this context, it is of paramount importance to find more combined therapies to optimize outcomes for patients with liver cancer.

Mesenchymal stem cells (MSCs), a major compartment of tumor microenvironment, can migrate to tumor sites and have been documented in HCC progression and metastasis (Thomas, 2014; Zhou, 2019). Bone marrow stem cells (BMSCs) can get into the liver and differentiate into epithelial cells, endothelial cells and myofibroblasts (Wright, 2002). BMSCs can differentiate into functional hepatocyte-like cells, which are assumed to be a potential option in regenerative medicine and clinical treatment of liver diseases (Zhang F., 2019). By the way, the metastasis of HCC requires liver cancer cells to escape apoptotic signals and host immune responses, and the support of intercellular communication in tumor microenvironment (Guo, 2011). Extracellular vesicles (EVs), including exosomes and microvesicles, contain mRNA, microRNAs (miRNAs), lipids, and proteins and have profound impacts on intercellular communication during normal physiology and pathological processes (Schorey, 2018; Tomarev, 2020). Many clinical researches indicate that the tumor-derived exosomes (TDE) and their contents have great potential as a diagnostic tool for prostate cancer and breast cancer (Song, 2014; Thomas, 2014). Importantly, exosomes derived from HCC stimulate metastasis of tumor cells which are short of capacity to spread to a specific organ (Ba, 2020). But the regulatory effects of liver cancer-derived EVs on fibroblastic differentiation of BMSCs and liver cancer metastasis remain unknown.

Furthermore, exosomal miRNAs are pivotal components in cancer initiation and progression (Sadeghizadeh, 2020). HCC cell-exosomal miRNAs are identified as reliable serum biomarkers for HCC (Baek, 2020). In the pre-experiment of this study, we found miR-181d-5p was the most upregulated in HepG2-EVs-treated BMSCs. However, its roles in hepatoma cell-derived EVs and in biological episodes in hepatoma cells are

not yet studied. We hypothesize that hepatoma cell-derived EVs promote liver cancer metastasis by inducing the differentiation of BMSCs through miR-181d-5p and underlying pathways. Microarray analysis, molecular and histochemical experiments were conducted to testify the involvement of hepatoma cell-derived EVs in cellular functions of liver cancer, which may shed novel insights for therapeutic interventions in the future.

MATERIALS AND METHODS

Ethics Statement

This study was ratified and supervised by the Ethics Committee of the Affiliated Hospital of Youjiang Medical University for Nationalities. All the guardians of the newborns signed the informed consent and knew the serum sample collection in this study. Great efforts were made to minimize the animals and their suffering.

BMSC Culture

Bone marrow mesenchymal stem cells were isolated from bone marrow of healthy volunteers ($n = 3$). Bone marrow samples (8–10 mL) were diluted with 10 mL phosphate buffer saline (PBS), centrifuged for 20 min at 500 g, and separated by density gradient method. The interface layer cells rich in nucleated cells were harvested and resuspended in Dulbecco's modified Eagle's medium (DMEM) with 10% fetal bovine serum (FBS) at 37°C with 5% CO₂. After 48 h, the culture media were changed to remove the non-adherent cells. The medium was then refreshed every 3 days. When the cell confluence reached 85–95%, cells were trypsinized, counted and seeded again. Cell morphology was observed under an optic microscope (Olympus Optical Co., Ltd, Tokyo, Japan). The cells at 3rd to 6th passage were selected for following experiments.

The hepatoma cell lines HepG2, Huh7, and H22 were obtained from the American type culture collection (ATCC, Manassas, VA, United States), and cultured in DMEM + 10% FBS at 37°C with 5% CO₂.

Evaluation of Differentiation Potency of BMSCs

For adipogenic differentiation, BMSCs were seeded in 24-well microplates at the concentration of 8×10^4 cells/well and cultured in the adipogenic differentiation medium for 21 days with the consumed medium refreshed every 3 days. Derived adipocytes were stained red with Oil Red O (Sigma-Aldrich, Merck KGaA, Darmstadt, Germany). For osteogenic differentiation, 4×10^4 BMSCs were seeded in 24-well microplates and cultured in the osteogenic differentiation

medium for 21 days with the consumed medium refreshed every 3 days. Derived osteocytes were stained positive for Alizarin Red (Sigma-Aldrich). For chondrogenic differentiation, 2×10^5 BMSCs seeded in a 24-well microplate were cultured with the chondrogenic differentiation medium for 21 days with the consumed medium refreshed every 3 days. Chondrocytes were stained positive with 1% toluidine blue (Sigma-Aldrich).

Flow Cytometry

BMSCs were detached with 0.25% trypsin, adjusted to 1×10^7 cells/mL, and incubated with monoclonal antibodies CD29, CD44, CD105, CD34, CD45, and human leukocyte antigen D-Related (HLA-DR) (Table 1) at 4°C for half an hour. After 1 × PBS wash, the positive rates were detected using a flow cytometer (MoFloastrios EQ, Beckman Coulter, CA, United States).

Apoptosis detection: after proper treatment, cells were washed in PBS and centrifuged at 2500 g to remove the supernatant, and then resuspended in the buffer solution and adjusted to 1×10^6 cells/mL. Subsequently, 500 μL cell suspension, 5 μL annexin V-fluorescein isothiocyanate and 10 μL propidium iodide (Invitrogen Inc., Carlsbad, CA, United States) were mixed and placed into each tube. After a 10 minute-incubation without light exposure, apoptosis was detected using a flow cytometer.

Isolation and Identification of EVs

HepG2 cells were cultured in DMEM/F12 with 100 IU/ml penicillin, 100 IU/ml streptomycin and 10% FBS without EVs (the EVs were depleted by centrifugation at 200,000 g for 18 h), and the supernatant was collected after centrifugation at 700 g for 10 min. The EVs were separated from the collected supernatant by differential ultracentrifugation, and the morphology of separated EVs was observed by transmission electron microscopy (Thermo Fisher Scientific Inc., Waltham, MA, United States). EVs were resuspended into 1 mL, and the size and concentration of EVs were determined by Nanosight tracking analysis using ZetaView PMX 110 (Particle Metrix, Meerbusch, Germany). Western bolt analysis was utilized to determine the specific markers (Table 2) of the EVs, and the conditioned medium (CM) supplemented with EV inhibitor GW4869 (MCE, Monmouth Junction, NJ, United States) served as the control. miR-181d-5p mimic, miR-NC, miR-181d-5p

TABLE 1 | Antibodies used in flow cytometry.

Antibody	No.	Dilution
CD29	ab179471	1:500
CD44	ab157107	1:1000
CD105	ab11414	1:1000
CD34	ab81289	1:1000
CD45	ab10558	1:100
HLA-DR	ab20181	1:100

HLA-DR, human leukocyte antigen D-Related. All antibodies were purchased from Abcam (Cambridge, MA, United States).

TABLE 2 | Antibodies used in Western blot analysis.

Antibody	No.	Dilution
α-SMA	ab32575	1:1000
Vimentin	ab8978	1:1000
β-actin	ab8277	1:1000
N-cadherin	ab76057	1:1000
E-cadherin	ab15148	1:500
Collagen I	ab34710	1:1000
Collagen III	ab7778	1:5000
FAK	ab40794	1:2000
p-FAK	ab81298	1:1000
Src	ab47405	1:1000
p-Src	ab40660	1:1000
SOCS3 CD63	ab16030 ab59479	1:1000 1:1000
CD81 TSG101	ab79559 ab30871	1:1000 1:1000
APOA2	ab92478	1:1000

α-SMA, alpha-smooth muscle actin; FAK, focal adhesion kinase; Src, steroid receptor coactivator; SOCS, suppressor of cytokine signaling.

inhibitor were synthesized by GeneChem (Shanghai, China). After transfection into HepG2 cells using Lipofectamine TM 2000 (Invitrogen), EVs were extracted and named EVs-mimic/EVs-negative control (NC)/EVs-inhibitor (inhi). The protein content of EVs was quantified by a Pierce bicinchoninic acid (BCA) protein determination kit (Beyotime, Jiangsu, China), and the result was 1.5 mg/mL. The protein content was used as the standard concentration.

Cell Treatment and Grouping

BMSCs were assigned into blank (normally cultured), CM-GW (incubated with the CM of HepG2 cells supplemented with GW4869), EVs (incubated with EVs at 5 μg or 50 μg protein content), EVs-NC (incubated with EVs-NC), EVs-mimic group (incubated with EVs-mimic), EVs-inhi (incubated with EVs-inhi), EVs/NC (incubated with EVs and transfected with pcDNA3.1 empty vector, Invitrogen), EVs/suppressors of cytokine signaling 3 (SOCS3) (incubated with EVs and transfected with SOCS3 overexpression vector), EVs/Y15 (incubated with EVs and treated with FAK inhibitor Y15), and EVs/PBS groups (incubated with EVs and treated with PBS of the equal volume of Y15). SOCS3 overexpression vector was constructed by cloning SOCS3 cDNA into pcDNA3.1, and Y15 was provided by MCE Inc.

Hepatoma cells (HuH7 or H22) were assigned into blank (normally cultured), CM (incubated with the CM of normally cultured BMSCs), CM-EVs (incubated with BMSCs in the EVs group), CM-EVs-NC (incubated with BMSCs in the EVs-NC group), CM-EVs-mimic (incubated with BMSCs in the EVs-mimic group), CM-EVs-inhi (incubated with BMSCs in the EVs-inhi group), CM-EVs/NC (incubated with BMSCs in the EVs/NC group), CM-EVs/SOCS3 (incubated with BMSCs in the EVs/SOCS3 group), CM-EVs/Y15 (incubated with BMSCs in the EVs/Y15 group), and CM-EVs/PBS groups (incubated with BMSCs in the EVs/PBS group).

Immunocytochemistry and Immunofluorescence

BMSCs were seeded into a culture dish with a coverslip. When the coverslip was mounted with cells, the culture solution was aspirated. Cells were washed in PBS, fixed in 4% formaldehyde for 15 min, and incubated for 20 min with 0.3% Triton-100. After PBS washes, cells were incubated in 1% bovine serum albumin (BSA) for 30 min and incubated with primary antibodies (Table 3) at 37°C for 1 h. Following 1 × PBS wash, cells were incubated with secondary antibody in a wet chamber for 30 min. Afterward, cells were washed with PBS again, visualized with 2,4-diaminobutyric acid, counterstained with hematoxylin, dehydrated and cleared, and observed under an optic microscope (Olympus Optical Co., Ltd, Tokyo, Japan).

BMSCs were cultured with the blocking buffer (PBS containing 5% normal goat serum, 3% BSA and 0.1% Triton-X 100) for 1 h, and then incubated with the primary antibody overnight. The cells were rinsed 3 min in PBS, incubated for 1 h with immunoglobulin G (IgG) (Alexa Fluor 488), and then counterstained with 4',6-diamidino-2-phenylindole (DAPI). When observing the internalization process, the EVs were incubated with Dil dye and then applied to BMSCs, and the cells were counterstained with DAPI. The above cells were photographed under the fluorescence microscope (Olympus).

Picric Acid-Sirius Red Staining

BMSCs were seeded onto the 6-well microplates at 1×10^5 cells/well overnight. On the second day, BMSCs were cultured with liver cancer-derived EVs for 48 h, fixed with 4% (m/v) paraformaldehyde for 30 min at room temperature, penetrated with 0.1% (v/v) Triton X-100, and washed with PBS. Then cells were stained with picric acid-Sirius red (0.1% Sirius red in saturated picric acid aqueous solution) (Beijing Solarbio Science & Technology Co., Ltd., Beijing, China) to detect collagen levels.

Western Blot Analysis

BMSCs were lysed in cold radio-immunoprecipitation assay containing a mixture of protease inhibitors (Sigma-Aldrich) for 30 min. Then, the lysate was centrifuged at 16000 g at 4°C for 20 min, and the supernatant was collected. The protein concentration was determined using a bicinchoninic

TABLE 3 | Antibodies used in immunocytochemistry and immunofluorescence.

Antibody	No.	Dilution
α-SMA	ab184675	1:100
vimentin	ab195877	1:1000
IgG	ab150117	1:200
collagen I	ab34710	1:1000
collagen III	ab7778	1:5000

α-SMA, alpha-smooth muscle actin; IgG, immunoglobulin G. All antibodies were purchased from Abcam (Cambridge, MA, United States).

acid assay kit (Beyotime, Jiangsu, China). Equal volume of samples (20 μL/well) was loaded onto sodium dodecyl sulfate-polyacrylamide gel electrophoresis. The proteins were subsequently transferred onto polyvinylidene fluoride membranes and then blocked with 5% fat-free milk for 1 h and probed with primary antibodies (Table 2) at 4°C overnight. After that, the membranes were incubated with secondary antibody IgG (1:2000, ab205718, Abcam). With β-actin as a control, protein bands were developed with enhanced chemiluminescence, and the signal intensity of target bands was analyzed using the Image J software.

Reverse Transcription Quantitative Polymerase Chain Reaction (RT-qPCR)

Total RNA of BMSCs was extracted using TRIzol method (Invitrogen) and the ultraviolet analysis and formaldehyde denaturing gel electrophoresis were employed to identify the high-quality RNA. RT-qPCR was performed as per the instructions of a RT-qPCR kit (Thermo Fisher Scientific). The primer sequences (Table 4) were synthesized by Shanghai Sangon Biotech Co., Ltd. (Shanghai, China). The relative expression was normalized by U6 or glyceraldehyde-3-phosphate dehydrogenase (GAPDH). Amplification and dissolution curves were determined after reaction, and fold change was calculated by $2^{-\Delta\Delta CT}$ method.

TABLE 4 | Primer sequences for RT-qPCR.

Gene	Primer sequence
α-SMA	F: 5'-CCCAAGACATCAGGGAGTAATGG3' R: 5'-TCTATCGGAACTTCAGCGTC-3'
Vimentin	F: 5'-CGTCCACACGCACCTACAG-3' R: 5'-GGGGGATGAGGAATAGAGGCT-3'
Collagen I	F: 5'-TAAGGGTCCCCATGGTGAGA-3' R: 5'-GGGTCCCTCGACTCTACAT-3'
GAPDH	F: 5'-GGGAGCCAAAAGGGTCA-3' R: 5'-GAGTCCTTCCACGATAACCA-3'
Collagen III	F: 5'-CTGTAACATGGAACTGGGGAAA-3' R: 5'-CCATAGCTGAACTGAAAACCACC-3'
SOCS3	F: 5'-ATGGTCACCCACAGCAAGTTCCC-3' R: 5'-TTAAAGGGGGCATCGTACTGGTC-3'
U6	F: 5'-CGCTTCGGCAGCACATATAC-3' R: 5'-AATATGGAACGCTTCACGA-3'
miR-21	F: 5'-TGTGGGTAGCTTATCAGAC-3' R: 5'-TGTCAAGACAGCCCCTCGACT-3'
miR-196a	F: 5'-TAGGTAGTTCATGTTGTTG-3' R: 5'-CCCAACAAACATGAAACTACC-3'
miR-222-3p	F: 5'-AGCTACATCTGGCTACTGGG-3' R: 5'-ACCCAGTAGCCAGATGTAGC-3'
miR-181d-5p	F: 5'-AACATTCAATTGTTGTCGGTG-3' R: 5'-ACCCACCGACAACAATGAAT-3'

RT-qPCR, reverse transcription quantitative polymerase chain reaction; α-SMA, alpha-smooth muscle actin; GAPDH, glyceraldehyde-3-phosphate dehydrogenase; miR, microRNA; F, forward; R, reverse.

3-(4, 5-Dimethylthiazol-2-yl)-2,5-Diphenyltetrazolium Bromide (MTT) Assay

The cells in the logarithmic growth stage were prepared into single cell suspension at 1×10^5 cells/mL, and then planted into 96-well microplates at 200 μL /well. At 12, 24, 36, and 48 h, the cell viability was added with 20 μL MTT (5 mg/mL, Sigma-Aldrich) to detect the viability. Dimethyl sulphoxide (DMSO) of 150 μL was added into each well to dissolve the crystal for 15 min. The absorbance (A) of each well was measured at 490 nm wavelength.

5-Ethynyl-2'-Deoxyuridine (EdU) Labeling Assay

According to the instructions of EdU cell proliferation kit (TransGen Biotech, Beijing, China), cells were incubated in complete media supplemented with 10 $\mu\text{mol/L}$ EdU at 37°C for 16 h. After PBS washing, cells were fixed and permeabilized, and stained with the reaction mixture and DAPI (Beyotime). Cell fluorescence was observed under the fluorescence microscope.

Transwell Assay

The invasion and migration of Huh7 and H22 cells were measured by Transwell assays. Huh7 and H22 cells were placed in the apical chamber of Transwell at 1×10^6 cells/mL, and the basolateral chamber was filled with complete media. The Transwell chamber was cultured for 24 h in serum-free DMEM at 37°C. The cells that were not on the surface of the filter were wiped out with cotton swabs, and the cells crossing the surface membrane of the filter were fixed with methanol and stained with 0.1% crystal violet. Cell migration was evaluated by counting in random fields of vision under the light microscope. For cell invasion assay, the same protocol was used, except that Matrigel (BD Bioscience, San Jose, CA, United States) was precoated on the filter membrane.

Microarray Analysis

The quantitative analysis of miRNAs was carried out by the affinity GeneChip miRNA array, and the miRNAs were labeled by the FlashTag Biotin HSR RNA labeling kit (Affymetrix Inc. Santa Clara, CA, United States). Samples were amplified and labeled with GeneChip WT PLUS kit (Affymetrix Inc.), and microarray hybridization. Washing and staining were performed with Fluidics Station 450 (Affymetrix Inc.). All steps were based on the process provided by Affymetrix. The data were analyzed by the expression console software of Affymetrix. The differential expression fold was set to be greater than 1.

Dual Luciferase Reporter Gene Assay

SOCS3 fragment containing miR-181d-5p binding site was cloned into pmirGLO disaccharidase vector (Promega, Madison, WI, United States) to construct pmirGLO-SOCS3-wild type (WT) reporter vector. The same fragment of SOCS3 except that the miR-181d-5p binding site was mutated was named pmirGLO-SOCS3-mutant (Mut). BMSCs were transfected with the constructed vectors, respectively, and then transfected with miR-181d-5p mimic and miR-NC, respectively. After

transfection for 48 h, the luciferase activity was determined with the determination system (Promega), and the relative activity was calculated as the ratio of luciferase activity of firefly to that of Renilla.

Animal Experiments

BALB/c nude mice obtained from Guangdong Medical Experimental Animal Center (license No. SCXK (Yue) 2018-0002) were raised in the specific pathogen-free environment, with free access to food and water. All the 72 nude mice were numbered according to their body weight, and randomly assigned into three groups using the random number method, with 24 mice in each group. In the blank group, 12 mice were injected subcutaneously with untreated Huh7 cells, and 12 mice with H22 cells, each mouse with 2×10^6 cells. In the CM group, 7 days after the treatment in the blank group, mice were treated with CM (100 μL) of BMSCs via the tail vein every 3 days. In the CM-EVs group, 7 days after the treatment in the blank group, mice were treated with CM (100 μL) of EVs-treated BMSCs via the tail vein every 3 days. The tumor volume and weight were recorded every 3 days. After 28 days, the mice were euthanized by intraperitoneal injection of excessive pentobarbital (Kopaladze, 2000; Reimer, 2017). The tumors were removed and weighed. Six tumors in each group were embedded in paraffin and sliced. The remaining 6 tumors were ground into homogenate for detecting protein expression.

In addition, another 9 nude mice were assigned into three groups, 3 in each group. Except that the mice were injected with luciferase-treated Huh7 cells through the tail vein, the other procedures were the same as those in the subcutaneous tumorigenesis treatment. On the 14th, 28th, 42nd, and 56th days after injection, the nude mice were bioluminescently imaged *in vivo*. After euthanasia in the same way on the 56th day, the lung tissue of nude mice was removed, embedded in paraffin and sectioned.

Bioluminescence Imaging

D-Luciferin (150 mg/kg, Promega) was administered intraperitoneally 5 min prior to imaging using an IVIS Spectrum (PerkinElmer, Inc. Waltham, MA, United States). Auto-exposure settings were used with a maximum exposure time of 1 min. Live image software version 4.4 (PerkinElmer, Inc. Waltham, MA, United States) was used to analyze bioluminescence signals. Standardized regions of interest were utilized to calculate average radiance (photons/second/cm²/steradian) across imaging sessions.

Histological Examination

Tissue sections were treated with Ki67 (1:500, ab15580, Abcam), N-cadherin (1:1000, ab76057, Abcam) and E-cadherin (1:500, ab15148, Abcam). The percentage of Ki67-positive cells was quantified by Image ProPlus 6.0. The lung sections of nude mice were dewaxed with xylene, washed with distilled water after hydration, and the metastasis was observed after hematoxylin and eosin (HE) staining.

Statistical Analysis

SPSS 21.0 (IBM Corp. Armonk, NY, United States) was employed for data analysis. The Kolmogorov-Smirnov test indicated whether the data were in normal distribution. The data were shown in the format of mean \pm standard deviation. The independent sample *t* test was used for comparisons between two groups, one-way analysis of variance (ANOVA) for comparisons among multiple groups, and Tukey's multiple comparison test for pairwise comparisons after ANOVA. The *p* value was calculated using a two-tailed test and *p* < 0.05 indicated a significant difference.

RESULTS

Identification of BMSCs and Hepatoma Cell-Derived EVs

Extracellular vesicles extracted from HepG2 cells were round and the diameter was about 100 nm (Figure 1A). The concentration of the extracted EVs was 4×10^6 particles/mL and the peak size was 110 ± 11 nm (Figure 1B). CD63, CD81, and TSG101 were all positive, and APOA2 was negative (Figure 1C).

BMSCs of the original generation were round and large in size. They began to attach after 24 h, and then became fusiform

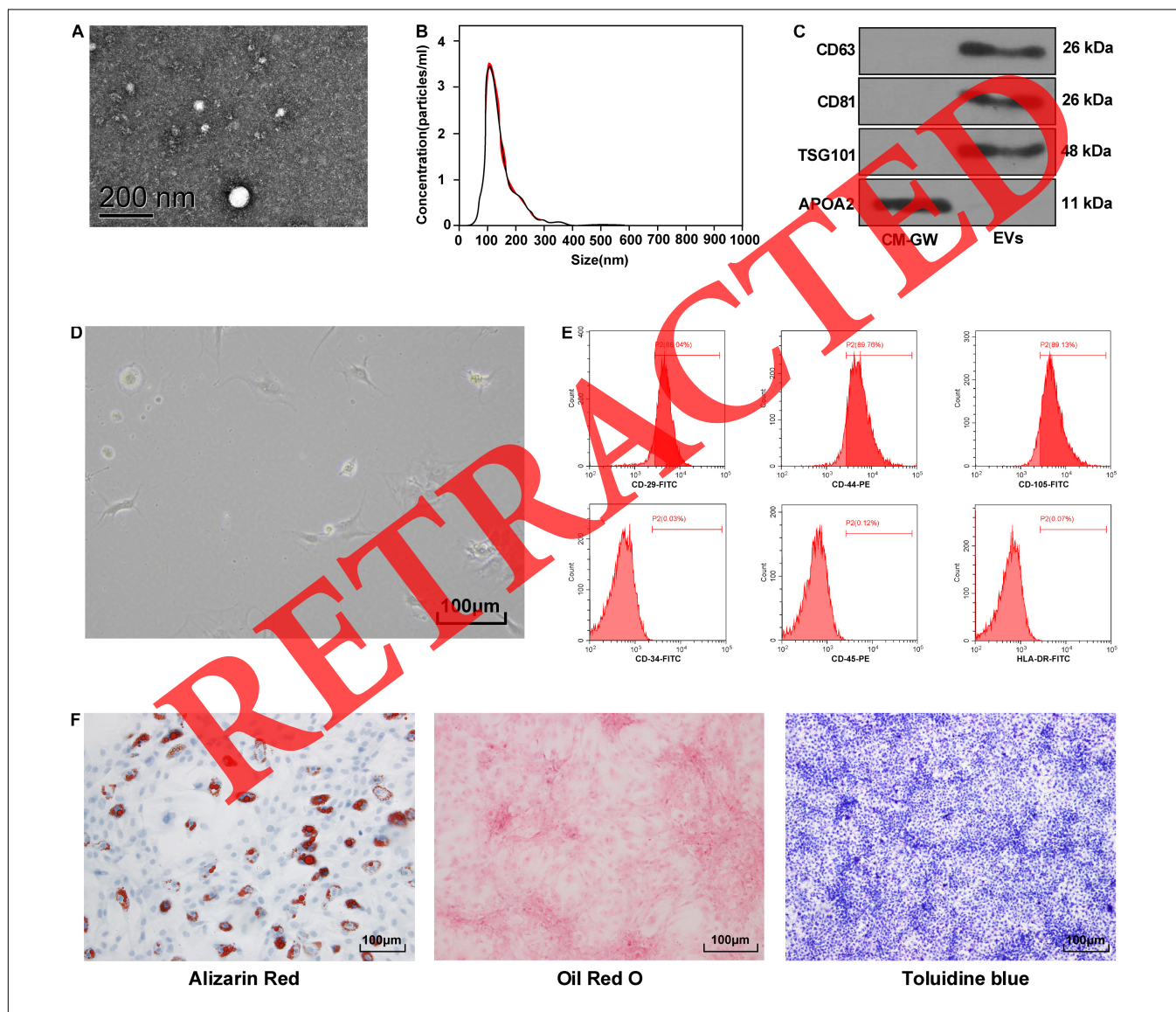


FIGURE 1 | Identification of BMSCs and hepatoma cell-derived EVs. **(A)** The morphology of EVs was observed by transmission electron microscopy. **(B)** The size and concentration of EVs were analyzed by nanoparticle tracking, the size was 110 ± 11 nm; the concentration was 4×10^6 particles/mL. **(C)** Western blot analysis detected the expression of specific marker proteins, and the conditioned medium of HepG2 cells treated with EV inhibitor GW4869 was used as the control. **(D)** The morphology of primary BMSCs was observed under an optic microscope. **(E)** The surface marker proteins of BMSCs was detected by flow cytometry, CD29/CD44/CD105 was positive, while CD34/CD45/HLA-DR was negative. **(F)** The differentiation potency of BMSCs was detected; from left to right, it is osteogenic differentiation, lipogenic differentiation, and chondrogenic differentiation. Stained color implied positive. Replicates = 3.

or polygonal (**Figure 1D**). Flow cytometry showed that BMSCs were highly positive for CD29, CD44, and CD105, but CD34, CD45, and HLA-DR were negative (**Figure 1E**). BMSCs also showed the ability to differentiate into osteoblasts, adipocytes, and chondrocytes (**Figure 1F**).

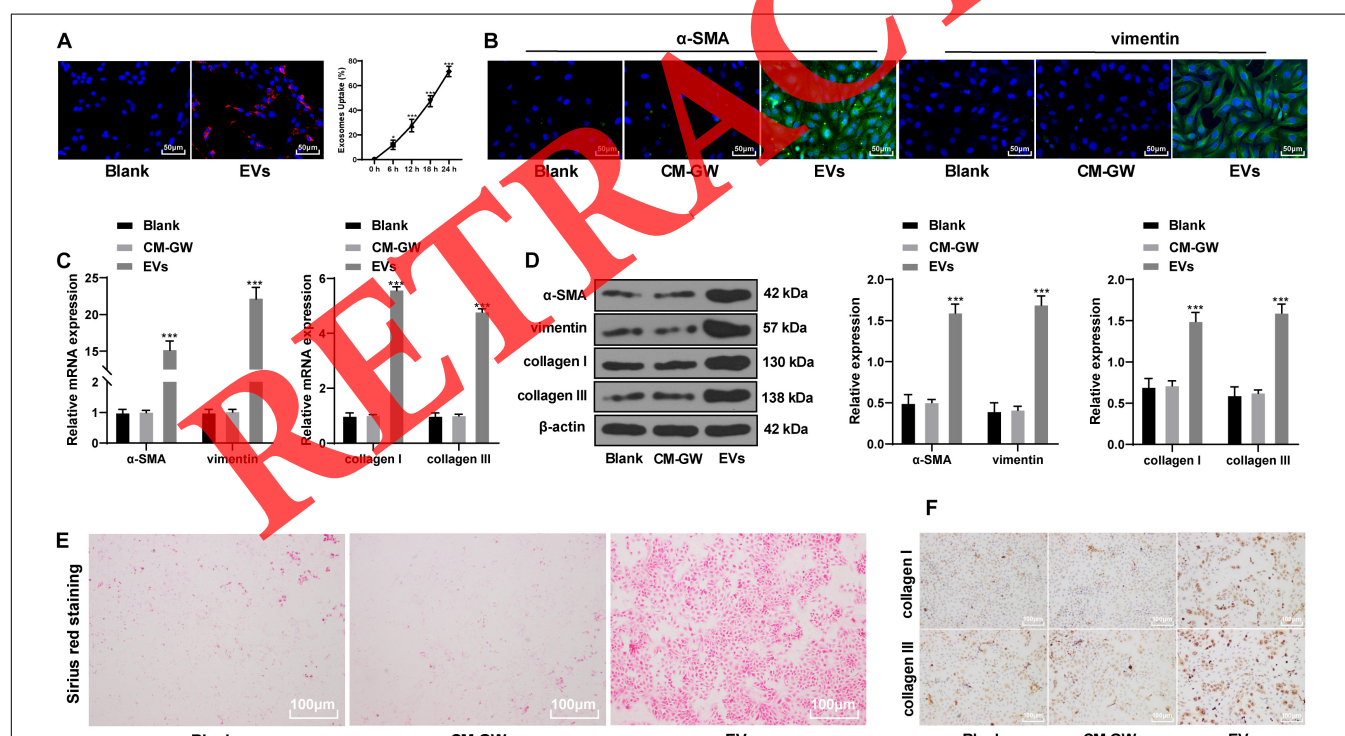
Hepatoma Cells-Derived EVs Promoted the Differentiation of BMSCs Into Fibroblasts

After incubation of EV isolated from hepatoma cells with BMSCs, the EVs were internalized by BMSCs, and the fluorescence increased gradually with increasing time (**Figure 2A**). Immunofluorescence (**Figure 2B**) and Western blot analysis (**Figure 2D**) indicated that the protein levels of alpha-smooth muscle actin (α -SMA) and vimentin in BMSCs treated with EVs were significantly elevated. After 48 h of treatment with EVs, the mRNA upregulation of α -SMA and vimentin was about 15 fold and 22 fold (**Figure 2C**) (all $p < 0.05$). Fibroblasts also express collagen (Jeffery, 2004), so we further determined the expression of collagen to reflect the fibroblast differentiation of BMSCs. Picric acid-Sirius red staining found that BMSCs treated with EVs had obvious collagen deposition (**Figure 2E**), and levels of type I collagen and type III collagen were also significantly enhanced (all $p < 0.05$; **Figures 2C–F**). It suggests

that the EVs derived from hepatoma cells promote fibroblastic differentiation of BMSCs.

BMSCs That Differentiated Into Fibroblasts After the Action of EVs Promoted EMT and Invasion and Migration of Hepatoma Cells

To observe the effect of fibroblastic differentiation of BMSCs on hepatoma cells, Huh7 and H22 cells were cultured in tumor cell growth medium (with 10% FBS) and the CM of BMSCs treated with different concentrations of EVs (1:1 in volume). The results of MTT and EdU experiments showed that compared with the CM group, BMSCs-CM treated with 50 μ g/mL EVs had a notable promoting effect on the proliferation of Huh7 and H22 cells ($p < 0.05$), while BMSCs-CM treated with 5 μ g/mL EVs had no significant effects ($p > 0.05$; **Figures 3A,B**). To eliminate the possible influence of FBS on cell proliferation, FBS concentration in the mixed media was reduced to 1%. Under the condition of 1% FBS, BMSCs treated with 50 μ g/mL EVs still promoted the proliferation of Huh7 and H22 cells (all $p < 0.05$; **Figure 3A**). BMSCs-CM treated with 50 μ g/mL EVs (CM-EVs) was selected for the subsequent experiments. CM-EVs significantly promoted the invasion and migration of Huh7 and H22 cells, and reduced the apoptosis rate (all $p < 0.05$;



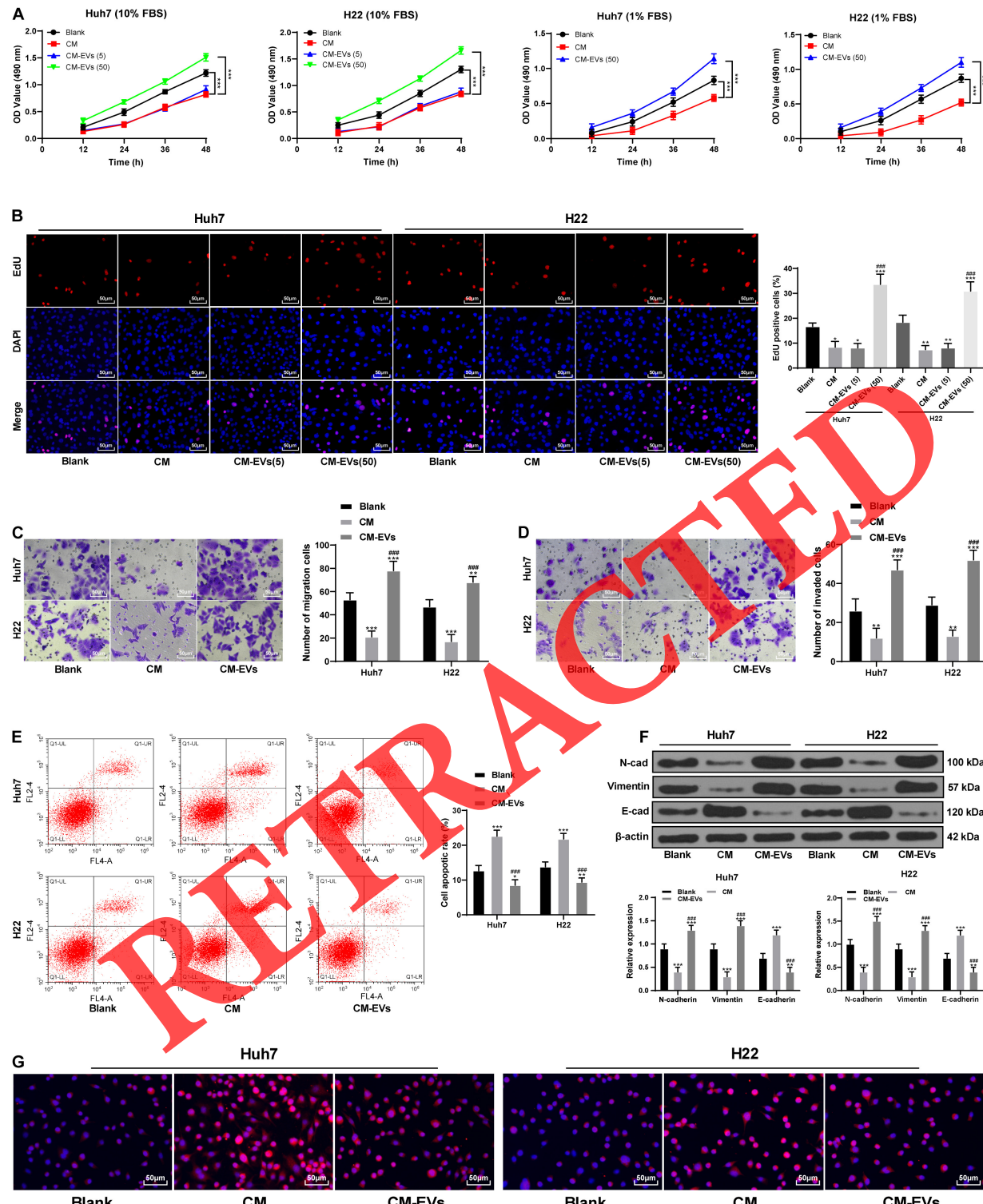


FIGURE 3 | BMSCs that differentiated into fibroblasts after the action of EVs promoted EMT and invasion and migration of Huh7 and H22 cells. MTT assay (**A**) and EdU assay (**B**) were used to detect the proliferation ability of Huh7 and H22 cells incubated with BMSCs-CM treated with different concentrations of EVs. (**C,D**) Transwell assays were used to detect the invasion and migration abilities of Huh7 and H22 cells incubated with CM-EVs. (**E**) Flow cytometry was used to detect the apoptosis rate of Huh7 and H22 cells incubated with CM-EVs. (**F**) Western blot analysis was used to detect the expression of EMT-related proteins in Huh7 and H22 cells incubated with CM-EVs. (**G**) Immunofluorescence was used to verify the positive expression of E-cadherin in Huh7 and H22 cells; compared with the blank group, * $p < 0.05$ ** $p < 0.01$, *** $p < 0.001$; compared with the CM group, ### $p < 0.001$. Data were analyzed by one-way ANOVA, followed by Tukey's multiple comparison test. Replicates = 3.

Figures 3C–E). CM-EVs elevated the expression of N-cadherin and vimentin in Huh7 and H22 cells and reduced E-cadherin expression (**Figure 3F**). Immunofluorescence staining further verified that CM-EVs markedly increased E-cadherin expression in hepatoma cells (**Figure 3G**). Briefly, BMSCs that differentiated into fibroblasts after the action of EVs can enhance the invasion and migration of hepatoma cells and promote EMT.

Hepatoma Cell-Derived EVs Carried miR-181d-5p Into BMSCs and Promoted Their Differentiation Into Fibroblasts

miRNAs are endogenous small non-coding RNAs, which can regulate gene expression and is related to tumorigenesis (Budhu,

2009). The differentially expressed miRNAs in BMSCs before and after the action of EVs were analyzed by miR microarray. The expression of miR-21, miR-196a, miR-222-3p, and miR-181d-5p was increased significantly in BMSCs after the action of EVs (**Figure 4A** and **Table 5**). The expression of these four miRNAs was verified by RT-qPCR. miR-181d-5p had the highest upregulation in BMSCs after the action of EVs ($p < 0.05$; **Figure 4B**), and its abundance in hepatoma cells-derived EVs was also the highest (**Figure 4C**). Therefore, we conclude that the HepG2-EVs may carry miR-181d-5p into BMSCs.

After miR-181d-5p mimic and inhibitor were utilized to up- or downregulate miR-181d-5p expression in HepG2 cells, and then EVs-mimic and EVs-inhi were extracted and applied to BMSCs. miR-181d-5p expression in the EVs and in EVs-treated

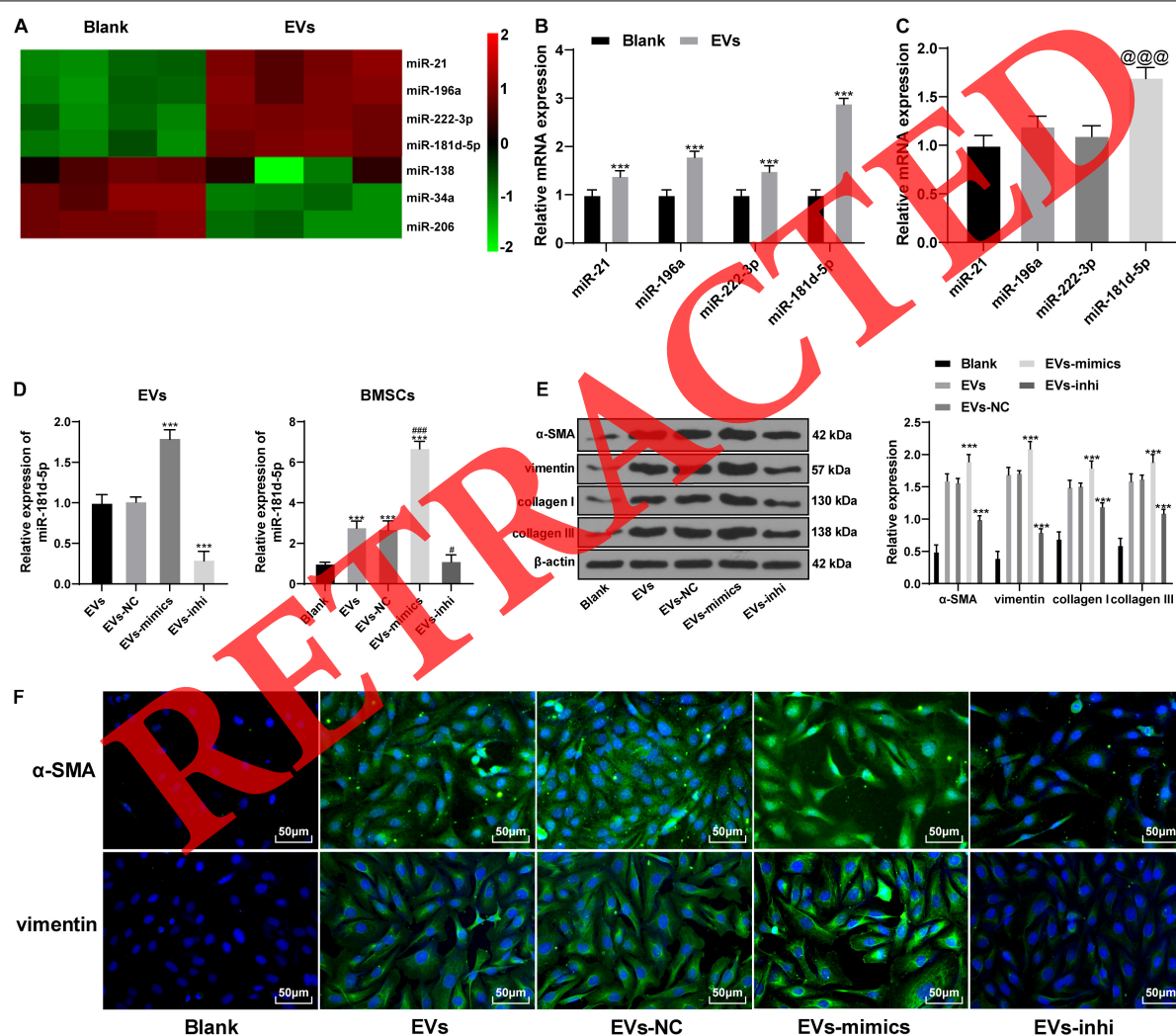


FIGURE 4 | Hepatoma cells-derived EVs promoted the differentiation of BMSCs by carrying miR-181d-5p into them. **(A)** The differentially expressed miRNAs in BMSCs before and after the action of EVs were analyzed by miR microarray. **(B,C)** miR expression in EVs-treated BMSCs (**B**) and in EVs (**C**); compared with the expression of miR-21 in EVs, the expression of miR-181d-5p was significantly increased, @@@ $p < 0.001$. **(D)** miR-181d-5p expression in EVs-mimic and EVs-inhi, and in BMSCs treated with EVs-mimic and EVs-inhi. **(E)** The levels of α-SMA, vimentin, collagen I, and collagen III in EVs-treated BMSCs were detected by Western blot analysis. **(F)** α-SMA and vimentin in EVs-treated BMSCs were detected by immunofluorescence. Compared with the blank group, *** $p < 0.001$; compared with the EVs group, # $p < 0.05$, ### $p < 0.001$. Data in panel **(B)** was analyzed by the *t* test, and data in panels C–E were analyzed by one-way ANOVA, followed by Tukey's multiple comparison test. Replicates = 3.

TABLE 5 | Results of miR microarray analysis.

miRNA	Fold change	Average expression	Adjusted P-value
miR-21	1.690	2.692	0.003
miR-196a	1.801	3.822	0.022
miR-222-3p	1.457	1.880	0.023
miR-181d-5p	2.929	2.236	0.000
miR-138	-2.107	2.524	0.005
miR-34a	-1.036	5.388	0.022
miR-206	-0.972	10.199	0.046

miR, microRNA.

BMSCs was significantly up- or downregulated (all $p < 0.05$; **Figure 4D**). Compared with the EVs group, the expression of α -SMA and vimentin in the BMSCs treated with EVs-mimic increased significantly, and the collagen deposition increased; while BMSCs treated with EVs-inhi showed opposite outcomes (all $p < 0.05$; **Figures 4E,F**). It suggests that the hepatoma cells-derived EVs can promote the differentiation of BMSCs by carrying miR-181d-5p into them.

BMSCs Treated With Downregulated miR-181d-5p in HepG2-EVs Reduced the EMT and Invasion of Hepatoma Cells

To further study the effect of miR-181d-5p on the differentiation of BMSCs and metastasis in the microenvironment of liver cancer, we applied EVs-mimic or EVs-inhi treated BMSCs-CM (CM EVs-mimic, CM-EVs-inhi) to Huh7 or H22 cells. Compared with the CM-EVs, Huh7, and H22 cells treated with CM-EVs-mimic had notably increased malignant episodes and N-cadherin and vimentin expression, and declined E-cadherin expression; while CM-EVs-inhi treatment showed opposite results (all $p < 0.05$; **Figures 5A–E**). The above results indicate that BMSCs treated with decreased miR-181d-5p expression in HepG2-EVs compromised the promoting effect of EVs-treated BMSCs on EMT and invasion and migration of hepatoma cells.

miR-181d-5p Carried by HepG2-EVs Targeted SOCS3 to Activate the FAK/Src Pathway

To study the downstream mechanism of miR-181d-5p, through online search and analysis of the database¹, we found that SOCS3 and miR-181d-5p had a targeted binding site (**Figure 6A**). Their targeting relationship was further verified by dual luciferase reporter gene assay (**Figure 6B**). In addition, levels of SOCS3 were decreased in BMSCs after the action of HepG2-EVs, and miR-181d-5p intervention in EVs-treated BMSCs inhibited SOCS3 expression (all $p < 0.05$; **Figures 6C–E**).

Activation of FAK/Src pathway can enhance cell motility and promote cell migration (El-Abhar, 2018). Levels of p-FAK and p-Src were increased in BMSCs treated with EVs ($p < 0.05$; **Figure 6E**). In conclusion, miR-181d-5p carried by HepG2-EVs can inhibit SOCS3 to activate the FAK/Src pathway and promote the differentiation of BMSCs.

¹<http://www.targetscan.org>

SOCS3 Overexpression Inhibited the FAK/Src Pathway and Reversed the Promotion of Invasion Induced by BMSCs That Differentiated Into Fibroblasts After the Action of EVs

To further confirm the above mechanism, we constructed an SOCS3 overexpression vector in the functional rescue experiment and transfected it into EVs-treated BMSCs (**Figures 7A,B**). SOCS3 overexpression reduced the fibroblast differentiation of BMSCs caused by HepG2-EVs, and reduced the phosphorylation of FAK and Src (**Figures 7C–E**). Then, BMSCs-CM with the overexpression of SOCS3 and EV treatment (CM-EVs/SOCS3) was applied to Huh7 and H22 cells. Compared with CM-EVs/NC treatment, CM-EVs/SOCS3 treatment inhibited the proliferation, invasion and migration abilities of Huh7 and H22 cells (all $p < 0.05$; **Figures 7E–H**). In addition, we also applied FAK inhibitor (Y15) to EVs-treated BMSCs, and then treated the hepatoma cells. The changes of invasion and migration abilities of hepatoma cells was similar to those with the above treatment of SOCS3 overexpression (all $p < 0.05$; **Figures 7E–H**). These results confirm that miR-181d-5p carried by HepG2-EVs could affect the differentiation of BMSCs, and the invasion and migration of hepatoma cells through SOCS3 and the FAK/Src pathway.

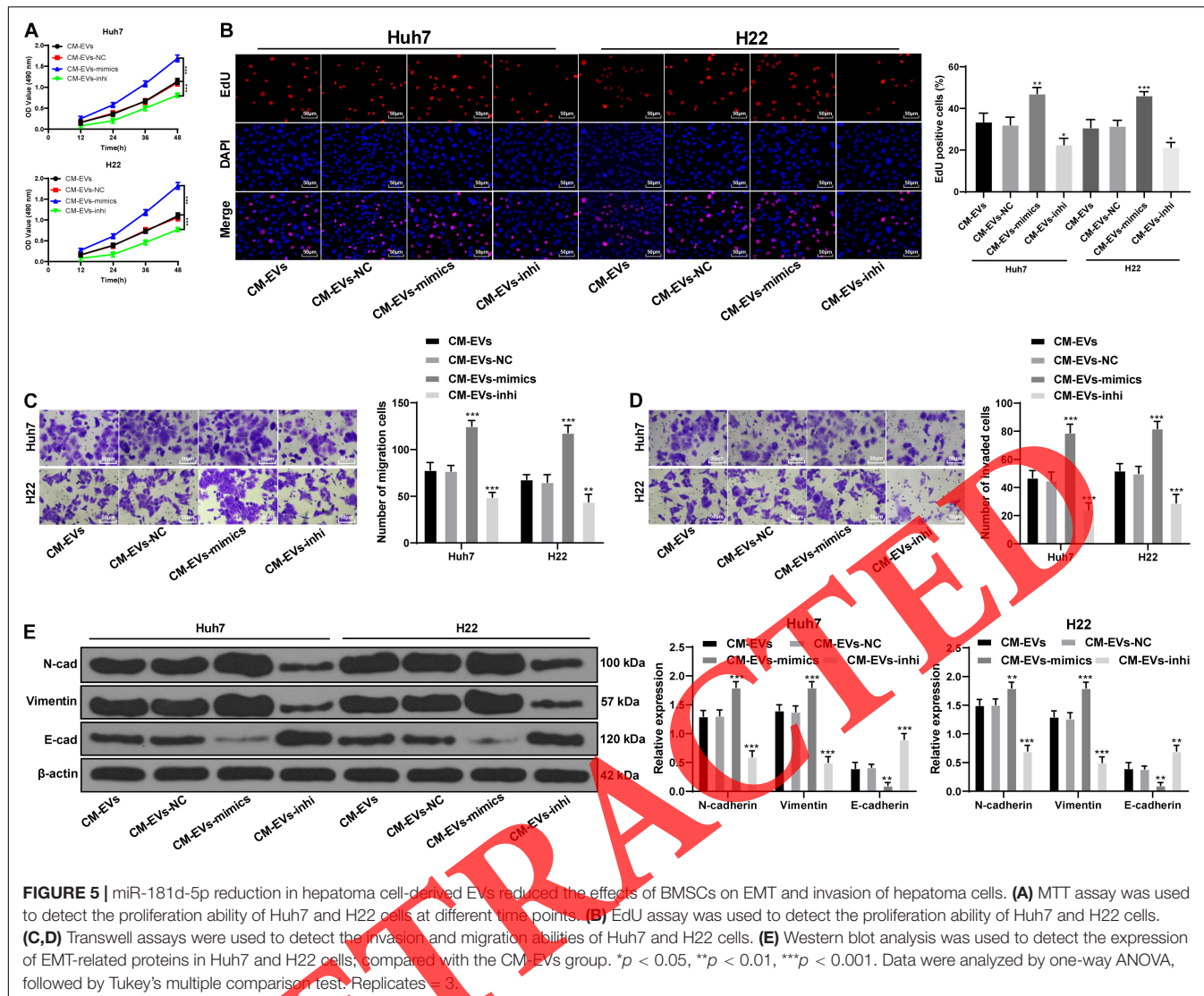
HepG2-EVs Undermined the Therapeutic Effect of BMSCs on the Tumor and Promoted Tumor Metastasis

In vivo, Huh7 and H22 cells were transplanted into the subcutaneous of nude mice to establish the subcutaneous tumor model. BMSCs-CM treated with EVs was injected into the tail vein. The tumor size and weight of CM-EVs-treated nude mice were higher than those of CM-treated mice (**Figures 8A,B**), and the positive rate of Ki-67 in tumors was enhanced significantly (**Figure 8C**). The expression of N-cadherin increased, and that of E-cadherin decreased (all $p < 0.05$; **Figure 8D**).

To better observe the effect of EVs-treated BMSCs on hepatoma metastasis, Huh7 cells transfected with luciferase were injected via the tail vein, and BMSCs-CM treated with different EVs was used for intervention. Through BLI imaging, we observed that the metastasis rate of hepatoma in the CM-EVs group was higher than that in the control group (**Figure 8E**); HE staining of lung tissue in the model nude mice showed that CM-EVs group had the highest lung metastasis rate (**Figure 8F**). Overall, hepatoma cell-derived EVs undermine the effect of BMSCs on tumor and promote tumor metastasis.

DISCUSSION

Despite the improvement in liver cancer in the last decades, the efficacy on this aggressive disease remains disappointing (Ding, 2016). Stem cells are a source of hepatocyte regeneration to repair the damaged liver, among which BMSCs have potential therapeutic value for liver diseases (Li, 2018). TDEs transfer the key factors from tumor cells to facilitate tumorigenesis, immune evasion and metastasis during HCC (Ba, 2020).

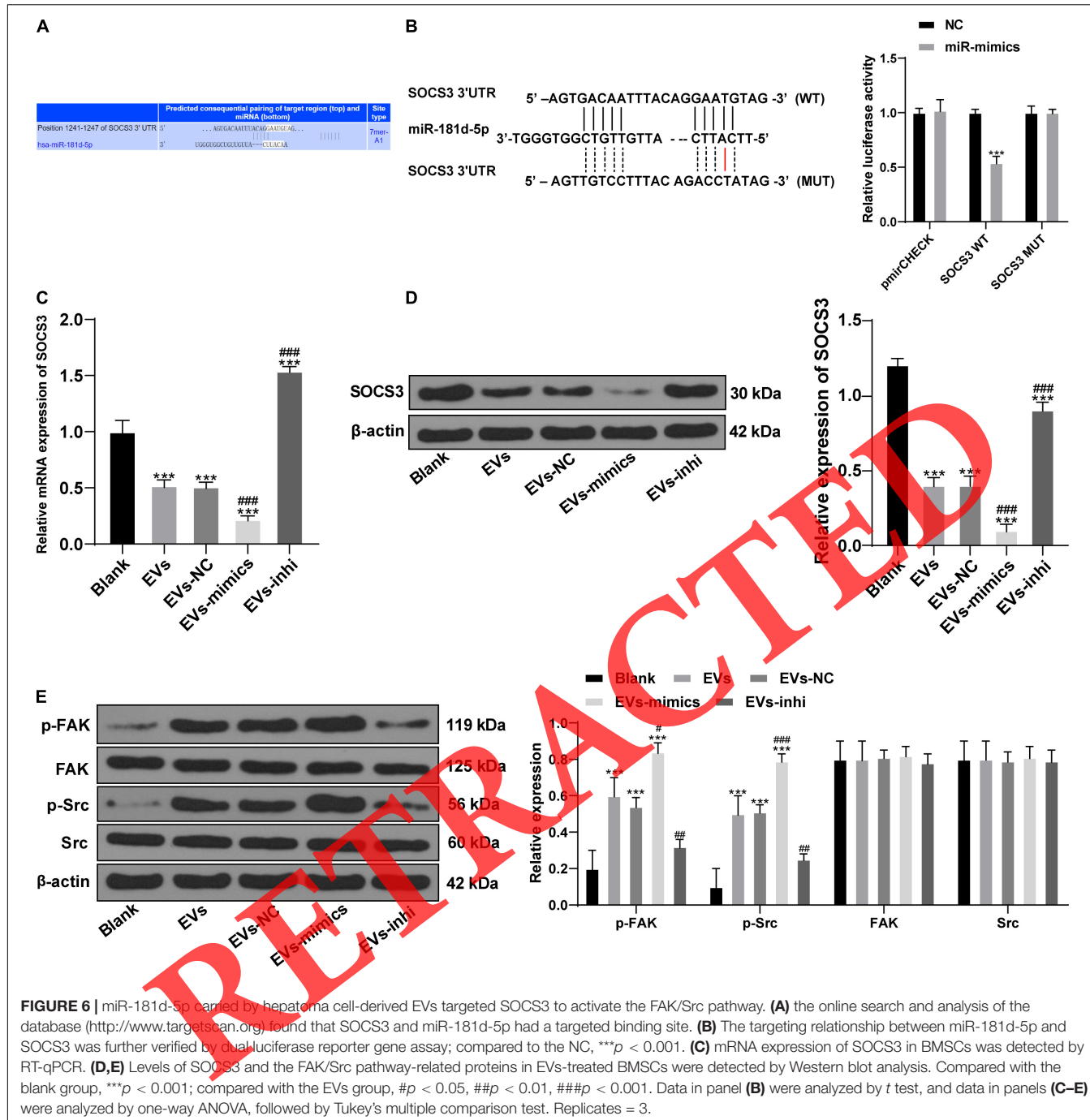


Importantly, BM progenitor cells may be influenced by exosomes (Lavotshkin, 2012). This rationale provided the framework for our investigation into the regulatory mechanisms underlying hepatoma cells-derived EVs in the effects of BMSCs on the metastasis of liver cancer. In this study, we highlighted the molecular mechanism that HepG2-EVs promoted the differentiation of BMSCs, and promoted liver cancer metastasis through the delivery of miR-181d-5p and the SOCS3/FAK/Src pathway. These findings might provide some new light for the treatment of liver cancer.

Microenvironmental elements are paramount at all steps of tumor invasion and metastasis and the recruitment of BMDCs, among which MSCs and exosomes derived from tumors are crucial for these processes (Pollard, 2009; Lavotshkin, 2012). In this study, EVs derived from hepatoma cells increased α -SMA and vimentin, and type I and type III collagen, thus promoting fibroblastic differentiation of BMSCs. The expression of α -SMA and vimentin are detected as

carcinoma-associated fibroblasts markers (Huang, 2020). Tumor microenvironment may trigger HCC initiation by recruiting BMSCs and subsequently stimulating their differentiation into fibroblasts, and promoting tumorigenesis (Zhang, 2013; Kawai, 2019). In the tumor microenvironment, TDEs promote the mobilization of BMDCs that supports tumor metastasis, and compromises the antitumor activities of BMSCs (Jia, 2012). In addition, BMSCs differentiated into fibroblasts after the action of HepG2-EVs-promoted EMT and invasion and migration of hepatoma cells. The first step of organotropic metastasis regulated by tumor exosomes is EMT, which is as a vital mechanism for epithelial cancer cells to acquire a malignant phenotype (Moller, 2013). TDEs contain plentiful amounts of EMT inducers, and endow EMT characteristics and the invasive and migratory capabilities to recipient cells, and contribute to metastatic environment (Sethi, 2016, 2019).

In Hep3B-EVs, 81 miRNAs are decreased by up to 205-fold compared to those in their donor cells (Lin, 2013).



miRNAs secreted by HCC exosomes may be a new direction for HCC targeted therapies through inactivation of oncogenic miRNAs (Ba, 2020). Our analyses indicated that HepG2-EVs promoted the differentiation of BMSCs by carrying miR-181d-5p. miR-181 is upregulated in an aggressive subgroup of HCCs and may contribute to HCC progression by targeting HCC cancer stem cells (Wang, 2011; Cancer Genome Atlas Research Network, 2017). miR-181d-5p participates in the development of osteosarcoma and breast cancer (Wang, 2020). However, the detailed mechanism of miR-181d-5p in liver cancer has not

been clarified. As our results demonstrated, BMSCs treated with HepG2-EVs with decreased miR-181d-5p expression impaired the promoting effect of EVs-treated BMSCs on EMT and invasion and migration of hepatoma cells. Similarly, cancer-associated fibroblast-derived exosomes promote EMT in breast cancer and the tumor growth by carrying miR-181d-5p (Wang, 2020). Tumor-derived exosomal miR-181-5p is adenocarcinoma-specific and its diagnostic accuracy has been verified (Chen, 2017). Likewise, it is reasonable to expect the diagnostic value of TDE-miR-181d-5p in liver cancer.

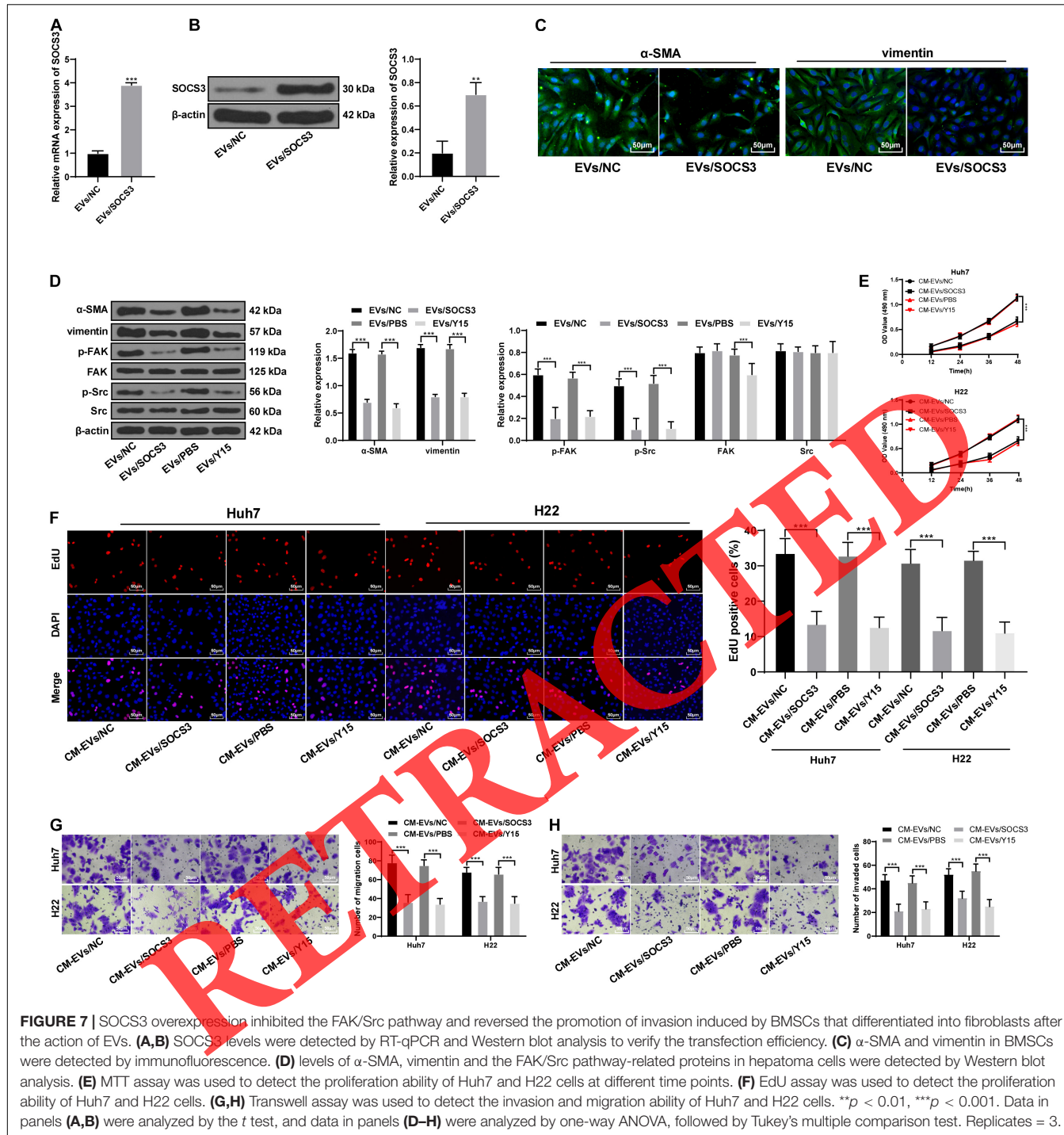
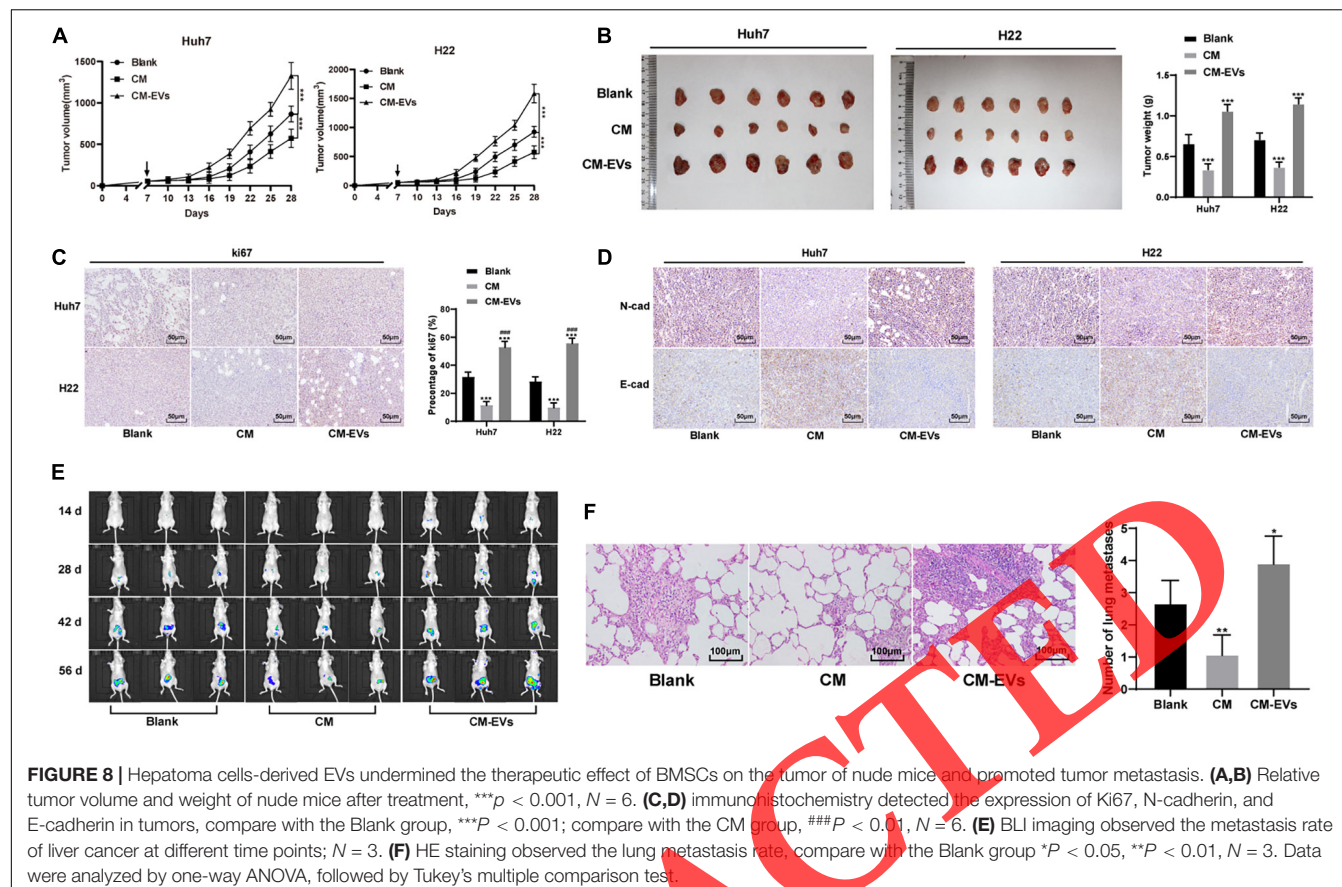


FIGURE 7 | SOCS3 overexpression inhibited the FAK/Src pathway and reversed the promotion of invasion induced by BMSCs that differentiated into fibroblasts after the action of EVs. **(A,B)** SOCS3 levels were detected by RT-qPCR and Western blot analysis to verify the transfection efficiency. **(C)** α-SMA and vimentin in BMSCs were detected by immunofluorescence. **(D)** levels of α-SMA, vimentin and the FAK/Src pathway-related proteins in hepatoma cells were detected by Western blot analysis. **(E)** MTT assay was used to detect the proliferation ability of Huh7 and H22 cells at different time points. **(F)** EdU assay was used to detect the proliferation ability of Huh7 and H22 cells. **(G,H)** Transwell assay was used to detect the invasion and migration ability of Huh7 and H22 cells. *** $p < 0.001$. Data in panels **(A,B)** were analyzed by the *t* test, and data in panels **(D–H)** were analyzed by one-way ANOVA, followed by Tukey's multiple comparison test. Replicates = 3.

Furthermore, we shifted to further investigating the downstream mechanism of miR-181d-5p in these events. Our results disclosed that miR-181d-5p carried by HepG2-EVs targeted SOCS3 to activate the FAK/Src pathway and promoted the differentiation of BMSCs. SOCS3 expression is lower in HCC tissue and negatively correlated with disease-free and disease-specific survival in HCC patients (Zhu, 2019). C-Src interacts with FAK and is highly expressed in HCC,

and activation of FAK/Src pathway enhances cell motility and promotes cell migration (El-Abhar, 2018). The functional rescue experiment verified that SOCS3 overexpression inactivated the FAK/Src pathway and reversed the promoting effect of HepG2-EVs-treated BMSCs on biological episodes of hepatoma cells. In HepG2 and Huh-7 cells, the overexpression of SOCS3 inhibits proliferation and invasion (Meng, 2019). Inhibition of Src/FAK pathway is a novel way for the synergistic effect of



rosuvastatin on the antitumor activities of dasatinib in HCC (El-Abhar, 2018). Restoration of SOCS3 in HCC cells inhibits the activation of FAK pathway, resulting in suppressed cell growth and migration (Shikauchi, 2005). Intriguingly, HCC-derived exosomes-mediated secretion of lysyl oxidase-like 4 promotes HCC metastasis by activating the FAK/Src pathway (Zhang X., 2019).

In the *in vivo* experiments, HepG2-EVs undermined the effects of BMSCs on tumor and promoted tumor metastasis. HCC-derived exosomes induce the intercellular crosstalk between tumor cells and fibroblasts, lead to increased vascular permeability, and facilitate lung and bone metastases (Lv, 2018). TDEs-treated bone marrows of mice have greater likelihood of tumor growth and lung metastases compared to that of control mice (Lavotshkin, 2012). The *in vivo* experimental results further supported the *in vivo* discoveries.

In summary, our study unveiled a novel role of hepatoma cells-derived EVs in the differentiation of BMSCs and liver cancer metastasis through the delivery of miR-181d-5p and the SOCS3/FAK/Src pathway. However, in the miR microarray analysis, we found several differentially expressed miRNAs (miR-21, miR-196a, and miR-222-3p) besides miR-181d-5p. They may also have potential participation in the complex efficacy of liver cancer-derived EVs and BMSCs in liver cancer. The downstream target gene of miR-181d-5p is more than SOCS3, and other tumor related genes may have played a role in our

research. We will make further investigation to testify their involvement in the future.

DATA AVAILABILITY STATEMENT

The original contributions presented in the study are included in the article/**Supplementary Material**, further inquiries can be directed to the corresponding authors.

ETHICS STATEMENT

The studies involving human participants and animal study were reviewed and approved by Ethics Committee of the Affiliated Hospital of Youjiang Medical University for Nationalities. The patients/participants provided their written informed consent to participate in this study.

AUTHOR CONTRIBUTIONS

HW, JW, ZX, and JP were the guarantors of integrity of the entire study and contributed to the manuscript preparation. HW and JP contributed to the study concepts, study design, definition of intellectual content, and literature research. HW, JW, ZX, JP, XL, and QT contributed to the manuscript editing and review,

and contributed to the data analysis and statistical analysis. HW, JW, ZX, WL, and JP contributed to the clinical studies. HW, JW, ZX, XW, CZ, YL, and JP contributed to the experimental studies and data acquisition. All authors read and approved the final manuscript.

FUNDING

This work was supported by Baise Scientific Research and Technology Planning Bureau (Grant No. BK20195405) and

Guangxi Natural Science Foundation of China (Grant Nos. 2019GXNSFBA245023 and 2020GXNSFAA259019). The funding body didn't participate in the design of the study and collection, analysis, and interpretation of data and in writing the manuscript.

REFERENCES

- Ba, Q. (2020). Hepatocellular carcinoma-derived exosomes in organotropic metastasis, recurrence and early diagnosis application. *Cancer Lett.* 477, 41–48. doi: 10.1016/j.canlet.2020.02.003
- Baek, G. O. (2020). Serum Exosomal MicroRNA, miR-10b-5p, as a Potential Diagnostic Biomarker for Early-Stage Hepatocellular Carcinoma. *J. Clin. Med.* 9:281. doi: 10.3390/jcm9010281
- Budhu, A. (2009). Identification of microRNA-181 by genome-wide screening as a critical player in EpCAM-positive hepatic cancer stem cells. *Hepatology* 50, 472–480. doi: 10.1002/hep.22989
- Cancer Genome Atlas Research Network. (2017). Comprehensive and Integrative Genomic Characterization of Hepatocellular Carcinoma. *Cell* 169, 1327–1341e23. doi: 10.1016/j.cell.2017.05.046
- Chen, H. (2017). Evaluation of Tumor-Derived Exosomal miRNA as Potential Diagnostic Biomarkers for Early-Stage Non-Small Cell Lung Cancer Using Next-Generation Sequencing. *Clin. Cancer Res.* 23, 5311–5319. doi: 10.1158/1078-0432.CCR-17-0577
- Ding, J. (2016). Characteristics of liver cancer stem cells and clinical correlations. *Cancer Lett.* 379, 230–238. doi: 10.1016/j.canlet.2015.07.041
- El-Abhar, H. S. (2018). Inhibition of SRC/FAK cue: A novel pathway for the synergistic effect of rosuvastatin on the anti-cancer effect of dasatinib in hepatocellular carcinoma. *Life Sci.* 213, 248–257. doi: 10.1016/j.lfs.2018.10.002
- Guo, W. (2011). Hypoxia-inducible microRNA-210 augments the metastatic potential of tumor cells by targeting vacuole membrane protein 1 in hepatocellular carcinoma. *Hepatology* 54, 2064–2075. doi: 10.1002/hep.24614
- Huang, T. (2020). CXCR4/TGF-beta1 mediated self-differentiation of human mesenchymal stem cells to carcinoma-associated fibroblasts and promoted colorectal carcinoma development. *Cancer Biol. Ther.* 21, 248–257. doi: 10.1080/15384047.2019.1685156
- Jeffery, R. (2004). Bone marrow contribution to tumor-associated myofibroblasts and fibroblasts. *Cancer Res.* 64, 8492–8495. doi: 10.1158/0008-5472.CAN-04-1708
- Jemal, A. (2018). Cancer statistics, 2018. *CA Cancer J. Clin.* 68, 7–30. doi: 10.3322/caac.21442
- Jia, J. (2012). Murine bone marrow stromal cells pulsed with homologous tumor-derived exosomes inhibit proliferation of liver cancer cells. *Clin. Transl. Oncol.* 14, 764–773. doi: 10.1007/s12094-012-0860-9
- Kawai, H. (2019). Differentiation and roles of bone marrow-derived cells on the tumor microenvironment of oral squamous cell carcinoma. *Oncol. Lett.* 18, 6628–6638. doi: 10.3892/ol.2019.11045
- Kontogiannis, V., and MacDaragh Ryan, P. (2020). Waist Circumference and Risk of Liver Cancer: A Systematic Review and Meta-Analysis of over 2 Million Cohort Study Participants. *Liver Cancer* 9, 6–14. doi: 10.1159/000502478
- Kopaladze, R. A. (2000). [Methods for the euthanasia of experimental animals—the ethics, esthetics and personnel safety]. *USP Fiziol. Nauk* 31, 79–90.
- Lavotshkin, S. (2012). Melanoma exosomes educate bone marrow progenitor cells toward a pro-metastatic phenotype through MET. *Nat. Med.* 18, 883–891. doi: 10.1038/nm.2753
- Li, X. (2018). A combination of ultrasound-targeted microbubble destruction with transplantation of bone marrow mesenchymal stem cells promotes recovery of acute liver injury. *Stem Cell Res. Ther.* 9:356. doi: 10.1186/s13287-018-1098-4
- Lin, W. L. (2013). Extracellular Vesicle-Mediated Transfer of a Novel Long Noncoding RNA TUC39: A Mechanism of Intercellular Signaling in Human Hepatocellular Cancer. *Genes Cancer* 4, 261–272. doi: 10.1177/1947601913499020
- Ly, G. (2018). Tumor-derived exosomal miR-1247-3p induces cancer-associated fibroblast activation to foster lung metastasis of liver cancer. *Nat. Commun.* 9:191. doi: 10.1038/s41467-017-02583-0
- Meng, X. (2019). Potential of C1QTNF1-AS1 regulation in human hepatocellular carcinoma. *Mol. Cell Biochem.* 460, 37–51. doi: 10.1007/s11010-019-03569-w
- Moller, A. (2013). The pre-metastatic niche: finding common ground. *Cancer Metastasis Rev.* 32, 449–464. doi: 10.1007/s10555-013-9420-1
- Pollard, J. W. (2009). Microenvironmental regulation of metastasis. *Nat. Rev. Cancer* 9, 239–252. doi: 10.1038/nrc2618
- Reimer, J. N. (2017). Refinement of intraperitoneal injection of sodium pentobarbital for euthanasia in laboratory rats (*Rattus norvegicus*). *BMC Vet. Res.* 13:60. doi: 10.1186/s12917-017-0982-y
- Rudolph, L., and Reddy, K. R. (2008). Diagnosis and treatment of hepatocellular carcinoma. *Gastroenterology* 134, 1752–1763. doi: 10.1053/j.gastro.2008.02.090
- Sadeghizadeh, M. (2020). microRNA-141-3p-containing small extracellular vesicles derived from epithelial ovarian cancer cells promote endothelial cell angiogenesis through activating the JAK/STAT3 and NF-kappaB signaling pathways. *J. Cell Commun. Signal.* 14, 233–244. doi: 10.1007/s12079-020-00548-5
- Schorey, J. S. (2018). Regulation and mechanisms of extracellular vesicle biogenesis and secretion. *Essays Biochem.* 62, 125–133. doi: 10.1042/EBC20170078
- Sethi, G. (2016). Exosome-Mediated Metastasis: From Epithelial-Mesenchymal Transition to Escape from Immunosurveillance. *Trends Pharmacol. Sci.* 37, 606–617. doi: 10.1016/j.tips.2016.04.006
- Sethi, G. (2019). Role of tumor-derived exosomes in cancer metastasis. *Biochim. Biophys. Acta Rev. Cancer* 1871, 12–19. doi: 10.1016/j.bbcan.2018.10.004
- Shikauchi, Y. (2005). Methylation silencing of SOCS-3 promotes cell growth and migration by enhancing JAK/STAT and FAK signalings in human hepatocellular carcinoma. *Oncogene* 24, 6406–6417. doi: 10.1038/sj.onc.1208788
- Singh, S. (2020). Challenges in liver cancer and possible treatment approaches. *Biochim. Biophys. Acta Rev. Cancer* 1873, 188314. doi: 10.1016/j.bbcan.2019.188314
- Song, J. (2014). A doxorubicin delivery platform using engineered natural membrane vesicle exosomes for targeted tumor therapy. *Biomaterials* 35, 2383–2390. doi: 10.1016/j.biomaterials.2013.11.083
- Thomas, R. (2014). Neoplastic reprogramming of patient-derived adipose stem cells by prostate cancer cell-associated exosomes. *Stem Cells* 32, 983–997. doi: 10.1002/stem.1619
- Tomarev, S. (2020). Extracellular vesicle therapy for retinal diseases. *Prog. Retin. Eye Res.* 2020:100849. doi: 10.1016/j.preteyes.2020.100849
- Wang, J. (2020). MicroRNA-181d-5p-Containing Exosomes Derived from CAFs Promote EMT by Regulating CDX2/HOXA5 in Breast Cancer. *Mol. Ther. Nucleic Acids* 19, 654–667. doi: 10.1016/j.omtn.2019.11.024
- Wang, X. W. (2011). Novel therapeutic strategies for targeting liver cancer stem cells. *Int. J. Biol. Sci.* 7, 517–535. doi: 10.7150/ijbs.7.517
- Wright, N. A. (2002). Hepatic and renal differentiation from blood-borne stem cells. *Gene. Ther.* 9, 625–630. doi: 10.1038/sj.gt.3301720

- Zhang, F. (2019). Microgravity-induced hepatogenic differentiation of rBMSCs on board the SJ-10 satellite. *FASEB J.* 33, 4273–4286. doi: 10.1096/fj.201802075R
- Zhang, J. (2013). Bone marrow mesenchymal stem cells in hepatocellular carcinoma. *Front. Biosci.* 18:811–819. doi: 10.2741/4145
- Zhang, X. (2019). Exosome-mediated secretion of LOXL4 promotes hepatocellular carcinoma cell invasion and metastasis. *Mol. Cancer* 18:18. doi: 10.1186/s12943-019-0948-8
- Zhou, Y. (2019). The hypoxia conditioned mesenchymal stem cells promote hepatocellular carcinoma progression through YAP mediated lipogenesis reprogramming. *J. Exp. Clin. Cancer Res.* 38:228. doi: 10.1186/s13046-019-1219-7
- Zhu, J. W. (2019). Expression and prognostic value of HER-2/neu, STAT3 and SOCS3 in hepatocellular carcinoma. *Clin. Res. Hepatol.* 43, 282–291. doi: 10.1016/j.clinre.2018.09.011

Conflict of Interest: The authors declare that the research was conducted in the absence of any commercial or financial relationships that could be construed as a potential conflict of interest.

Copyright © 2021 Wei, Wang, Xu, Li, Wu, Zhuo, Lu, Long, Tang and Pu. This is an open-access article distributed under the terms of the Creative Commons Attribution License (CC BY). The use, distribution or reproduction in other forums is permitted, provided the original author(s) and the copyright owner(s) are credited and that the original publication in this journal is cited, in accordance with accepted academic practice. No use, distribution or reproduction is permitted which does not comply with these terms.

RETRACTED